Electronic Supplementary Material (ESI) for Inorganic Chemistry Frontiers.

Supplementary Information

A Selenium-Based "Alkahest": Reactive Dissolutions of Metals and Metal Compounds with n-Alkylammonium Polyselenide Solutions

Jonathan W. Turnley,[a] Swapnil D. Deshmukh,[a] Victoria M. Boulos,[b] Robert Spilker,[a] Christian J. Breckner,[a] Kevin Ng,[a] Judy Kuan-Yu Liu,[b] Jeffrey T. Miller,[a] Hilkka I. Kenttämaa,[b] and Rakesh Agrawal[a,*]

[a]Davidson School of Chemical Engineering, Purdue University, West Lafayette, Indiana 47907, United States
[b]Department of Chemistry, Purdue University, West Lafayette, Indiana 47907, United States
*Email: agrawalr@purdue.edu

Representative Collision-Activated Dissociation Tandem Mass Spectra

Collision-activated dissociation (CAD) was used to help identify the elemental compositions of anions detected in negative-ion mode ESI/MS analysis. Both the indium polyselenide complexes and the copper polyselenide complexes, when isolated and subjected to CAD, underwent losses of selenium atoms. Representative spectra are shown in Figure S1 and Figure S2.

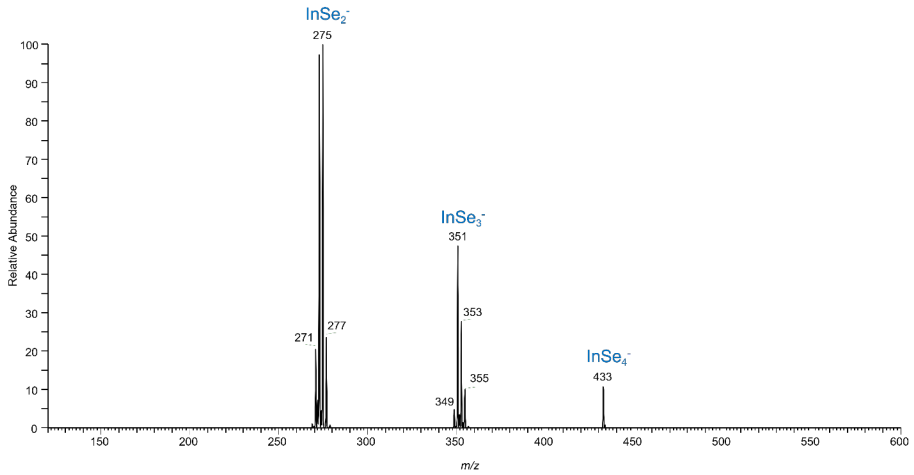

Figure S1. The low-resolution (-) ESI CAD tandem mass spectrum of the ions of m/z 433 measured at a nominal collision energy of 25.

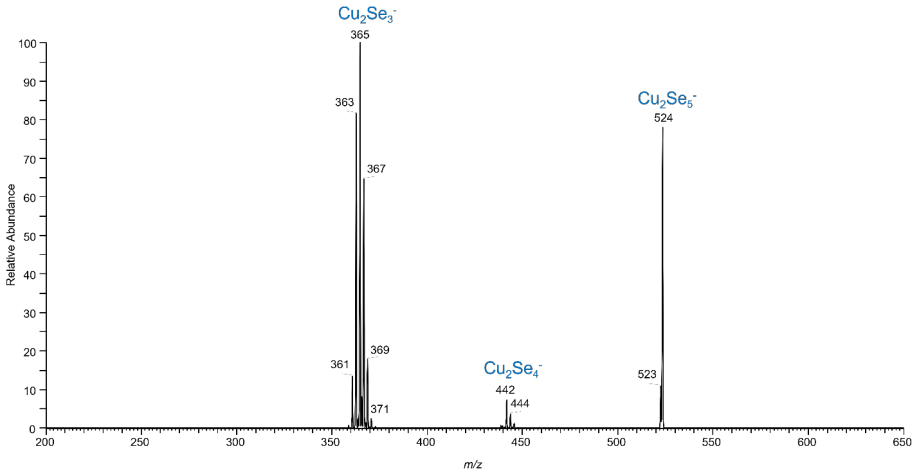

Figure S2 The low-resolution (-) ESI CAD mass spectrum of the ions of m/z 524 measured at a nominal collision energy of 15.

Extended Raman Spectrum of BAPSe

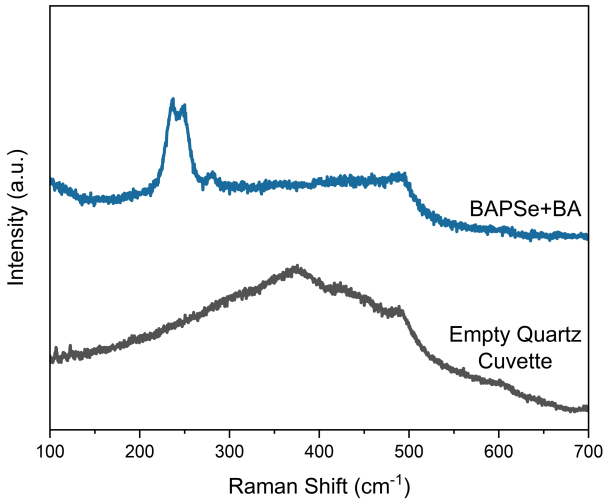

Figure S3. Raman spectra for BAPSe dissolved in BA showing no evidence of S-S, C-S, or S-Se vibrations at higher Raman shifts.

Expansion of the Polyselenide System

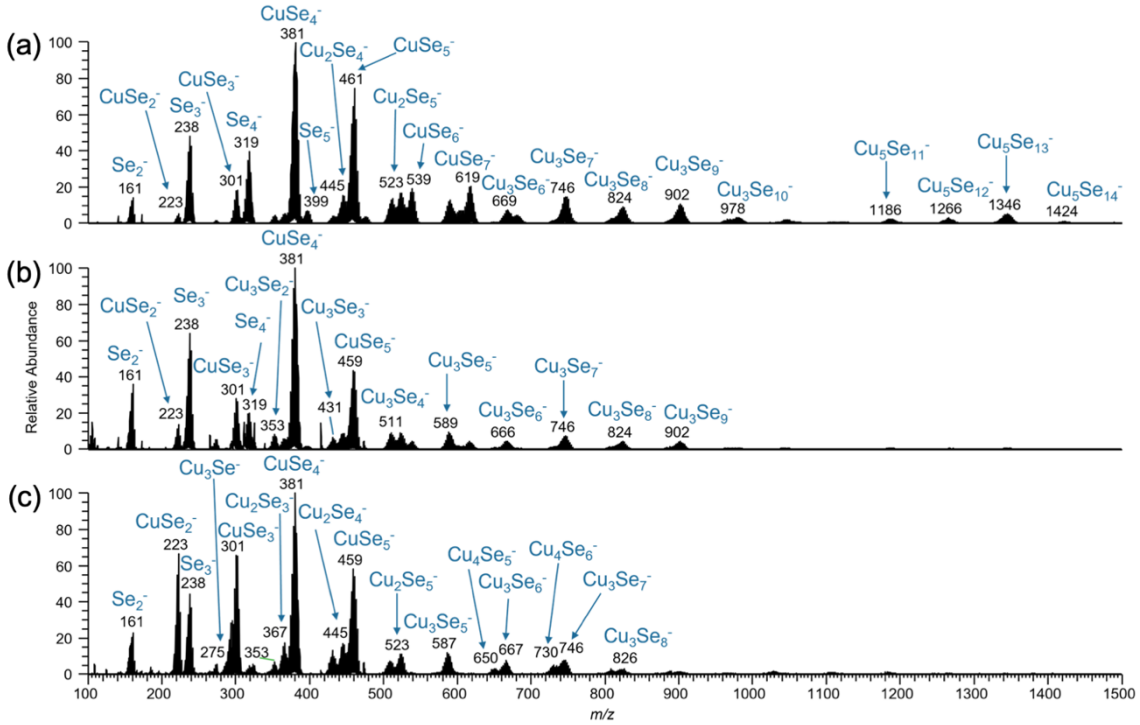

Figure S4. Negative-ion mode ESI/MS spectra of solutions obtained using BAPSe+BA to dissolve a) Cu_2Se, b) Cu_2O, and c) CuCl.

Given the ability of BAPSe to solubilize copper and indium, investigations were undertaken to assess the scope of these reactions for other copper and indium precursors. Cu_2Se was found to react BAPSe and get dissolved in n-butylamine. ESI-MS analysis suggests the formation of copper polyselenides (Figure S4). Cu_2O and CuCl were also found to be dissolved with BAPSe in butylamine, and ESI-MS analysis showed the formation of copper polyselenides. Interestingly, In_2Se_3 was found to be unreactive toward BAPSe.

To determine whether otherwise soluble salts still react with the polyselenides, dissolution of $InCl_3$ in DMF with and without BAPSe was studies. The dissolution of $InCl_3$ in BAPSe+DMF was noticeably different than the previously mentioned experiments for copper and indium compounds. A black solid was formed and identified through XRF and XRD as elemental selenium. $InCl_3$ is soluble in DMF and the Raman spectrum (Figure S5) of this solution shows a clear In-Cl peak at 294 cm^{-1}. On the other hand, when BAPSe was present, this In-Cl peak was no longer present and peaks at 173 cm^{-1} and 190 cm^{-1} appeared which can be attributed to In-Se bonding. Interestingly, the 190 cm^{-1} peak has not been previously seen in the indium polyselenide complexes in this work but was detected as the primary peak in the $[In_2Se_4]^{2-}$ complexes produced by hydrazine dissolutions of In_2Se_3 and Se.[1] These findings suggest that a different indium-selenium complex was formed. The difference in reactions could be related to starting with an oxidized indium source. If smaller selenium chains are needed to form the stable complexes, but there is no source of electrons from metal oxidation, the breaking of the polyselenide chain could produce one polyselenide ion and elemental selenium.

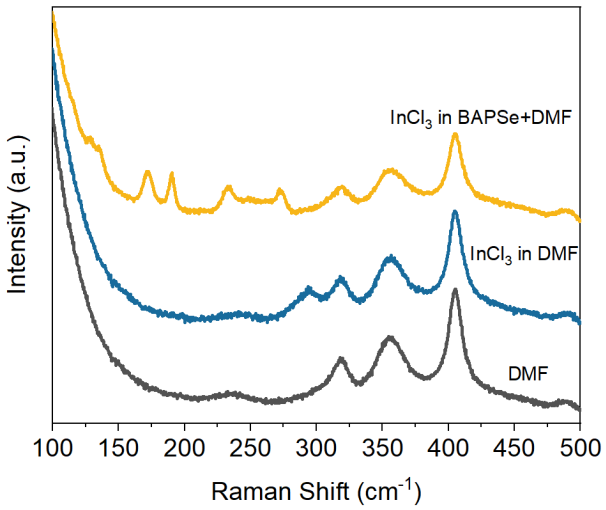

Figure S5. Raman spectra for $InCl_3$ dissolved in DMF with and without the presence of BAPSe.

In addition to investigating the copper or indium source, various cations for the alkylammonium polyselenide were used to dissolve copper metal. It was found in previous work that the cation size in the final metal polyselenide plays a role in stabilizing the structure.[2] Both n-propylammonium polyselenide and n-hexylammonium polyselenide were prepared through the dissolution of selenium in ethanethiol and n-propylamine or n-hexylamine, followed by precipitation with a nonpolar antisolvent. Both polyselenides completely dissolved copper metal at a selenium to metal ratio of 10:1.

Beyond the use of n-alkylamines, the dissolution of selenium in hydrazine produces hydrazinium polyselenide. Similar to alkylammonium polyselenides, we observed the presence of two Raman peaks attributed to Se-Se bonding (Figure S6), indicating the presence of longer and shorter polyselenide ions. We found that this hydrazinium polyselenide could facilitate the dissolution of indium metal. Interestingly, we again observed a reduction in the size of the peak attributed to longer polyselenide ions. This finding provides further support for the hypothesis that the oxidation of metals is linked with the breaking of polyselenide chains in this reactive dissolution.

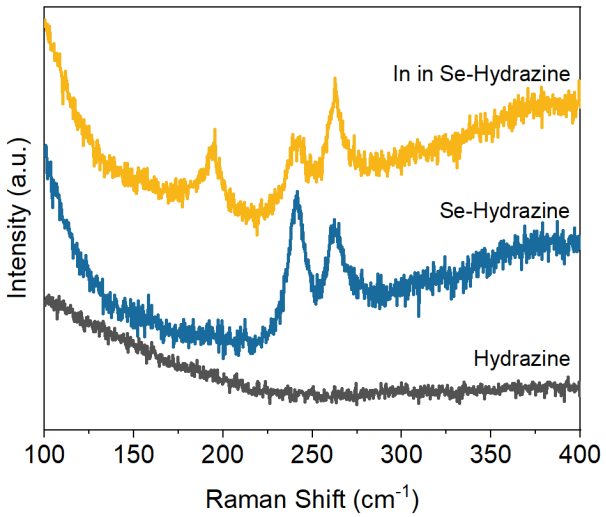

Figure S6. Raman spectra for selenium dissolved in hydrazine and indium metal dissolved in a selenium-hydrazine solution.

Representative Positive-Ion Mode ESI Mass Spectra

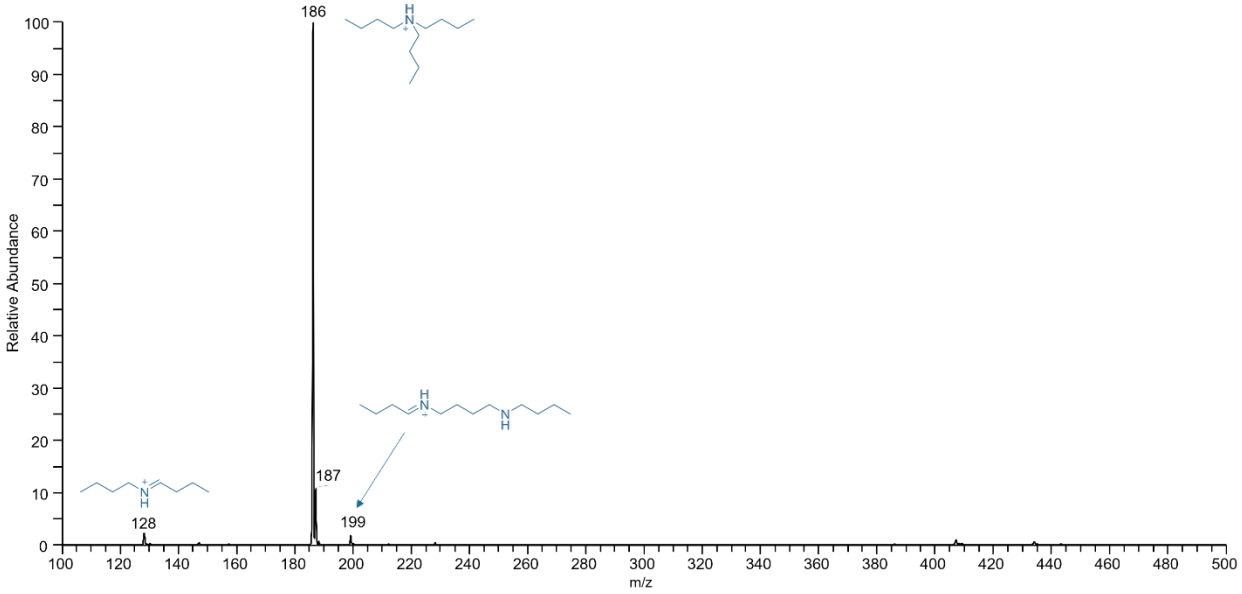

Figure S7. The low-resolution (+) ESI mass spectrum of the solution obtained using BAPSe+BA to dissolve In metal.

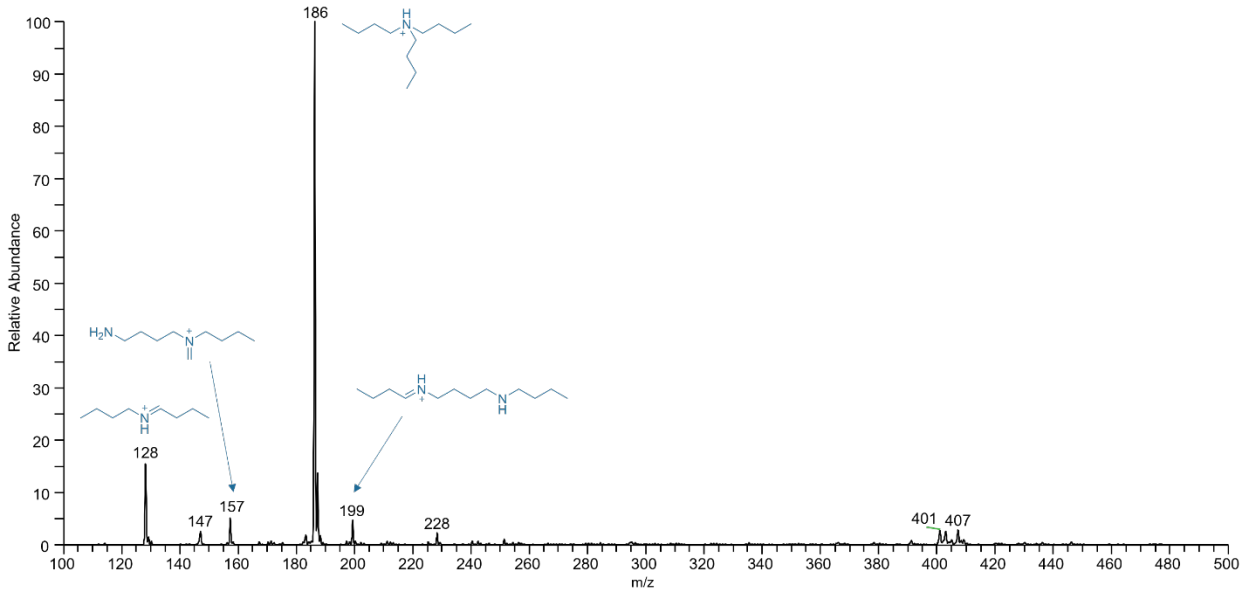

Figure S8. The low-resolution (+) ESI mass spectrum of the solution obtained using BAPSe+BA to dissolve Cu metal.

Raman Analysis of Dissolutions

The reduction in the lower Raman shift peak related to Se-Se bonding could be indicative that the oxidation of metals in alkylammonium polyselenide dissolution occurs due to electrons moving to the polyselenide ions and breaking one larger polyselenide chain into two smaller chains. While this observation in the Raman spectrum is easily seen in indium dissolutions, it is also present for other metals (Figure S9). Note the slight shift in intensities of the Se-Se peaks after silver is dissolved. While the change is less dramatic than when indium is dissolved in BAPSe+BA, this could be attributed to the lower solubility of silver metal in these solutions and the lower oxidation state, resulting in fewer electrons shared between more polyselenide ions. This trend is also observed in the case of copper dissolution in BAPSe+BA. The presence of a shoulder to the right side of the Se-Se peak at approximately 260 cm^{-1} may be indicative of Cu-Se bonding.

Elemental selenium can also be dissolved by BAPSe+BA. Rather than a metal being oxidized as part of its reactive dissolution, a chalcogen could potentially be reduced as part of a reactive dissolution. We see evidence of this as the opposite trend is observed regarding the selenium peaks (Figure S10). The peak at lower Raman shift, which would correspond to longer

polyselenide chain lengths increases relative to the peak at higher Raman shift. This could indicate the elemental Se is being added to the polyselenide ions, growing the size of the ions.

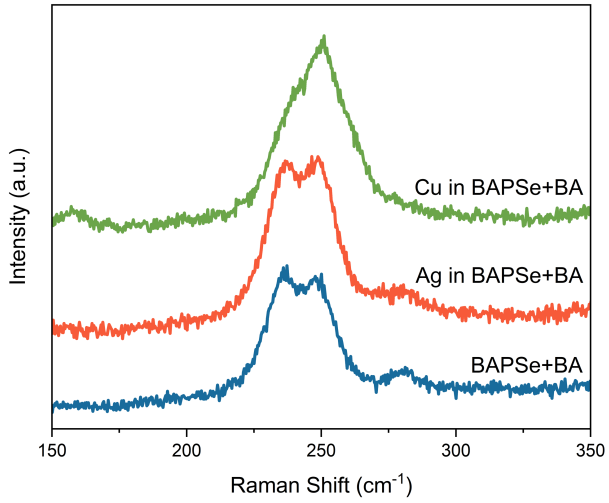

Figure S9. Raman spectra for BAPSe+BA, Ag dissolved in BAPSe+BA, and Cu dissolved in BAPSe+BA.

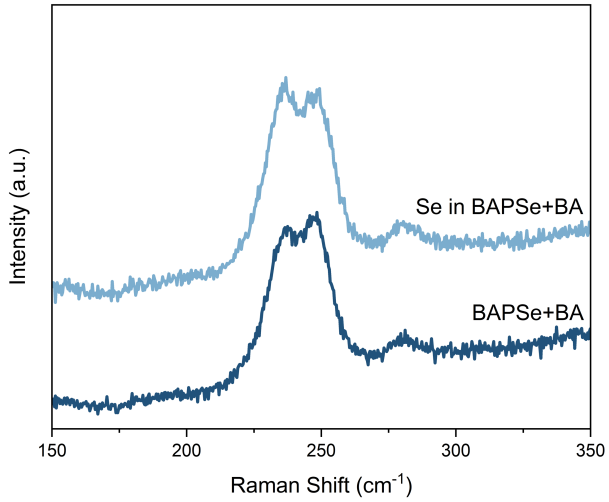

Figure S10. Raman spectra for BAPSe+BA and Se dissolved in BAPSe+BA.

XAS Analysis

Table S1. Structural Parameters Obtained from the Best Fits of Spectra from Metal Foils and Metals in BAPSe Solutions

Sample	Edge Energy (keV)	Scattering Pair	Coordination Number (±10%)	Bond Distance (±0.02 Å)	σ^2 (Å^2)	E_0 Shift
In K Edge						
In Foil	27.9273	In-In	12	3.21	0.025	1.1
In_2O_3	27.9404	In-O	6.4	2.16	0.0040	0.3
In in BAPSe+BA	27.9417	In-Se	5.8	2.58	0.0040	2.6
Cu K Edge						
Cu Foil	8.9790	Cu-Cu	12	2.53	0.0080	2.6
CuCl	8.9816	Cu-Cl	3.9	2.28	0.0140	-1.4
CuO	8.9835	Cu-O	3.8	1.96	0.0070	3.2
Cu in BAPSe+BA	8.9809	Cu-Se	3.7	2.34	0.0070	2.1
Se K Edge						
BAPSe+BA	12.6574	Se-Se	1.4	2.35	0.0020	0.0020
In in BAPSe+BA (Se/In = 7.79 ± 0.12)	12.6576	Se-Se	1.2	2.34	0.0020	0.0020
		Se-In	0.5	2.58	0.0020	0.0020
In in BAPSe+BA (Se/In = 6.38 ± 0.04)	12.6575	Se-Se	1.0	2.32	0.0020	0.0020
		Se-In	0.6	2.59	0.0020	0.0020

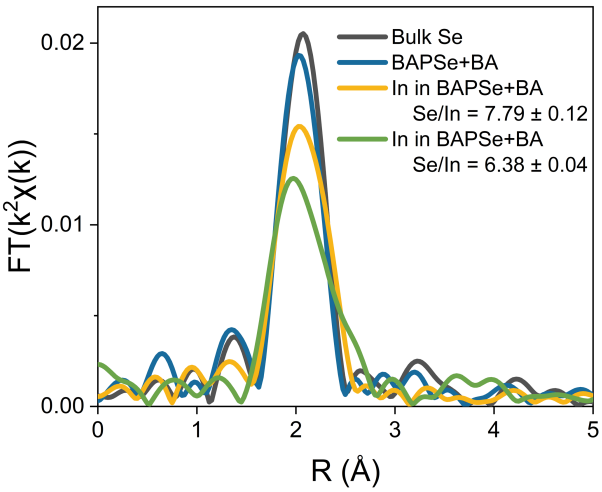

Figure S11. EXAFS spectra at Se K edge comparing elemental Se, BAPSe+BA, and In in BAPSe+BA at two different ratios.

Current-Voltage and Photoluminescence Characterization of $CuInSe_2$ Solar Cells

Table S2. Current-Voltage Analysis of $CuInSe_2$ Solar Cells from Cu-In-BAPSe Ink

Cell	Efficiency (%)	Voc (V)	Jsc (mA/cm^2)	FF (%)	Cell	Efficiency (%)	Voc (V)	Jsc (mA/cm^2)	FF (%)
A1	5.80	0.39	33.2	44.8	B2	7.25	0.38	37.4	50.8
A2	5.28	0.37	31.3	45.6	B3	6.39	0.37	35.6	48.4
A3	5.24	0.37	28.0	50.6	B4	6.51	0.38	32.0	53.5
A4	6.94	0.38	33.3	54.8	B5	7.02	0.38	34.5	53.5
A5	6.72	0.38	33.7	52.4	B6	7.23	0.38	35.3	53.9
A6	7.01	0.37	33.0	57.4	B7	7.11	0.37	34.0	56.4
A7	6.35	0.38	32.4	51.4	B8	5.79	0.37	30.1	51.9
A8	5.99	0.37	31.6	51.3	B9	6.93	0.38	34.4	53.1
A9	6.67	0.37	30.9	58.3	B10	6.61	0.38	34.0	51.1
A10	5.81	0.36	31.1	51.9	B11	7.06	0.38	34.9	53.2
B1	6.81	0.4	35.9	47.5	B12	6.54	0.38	31.7	54.4

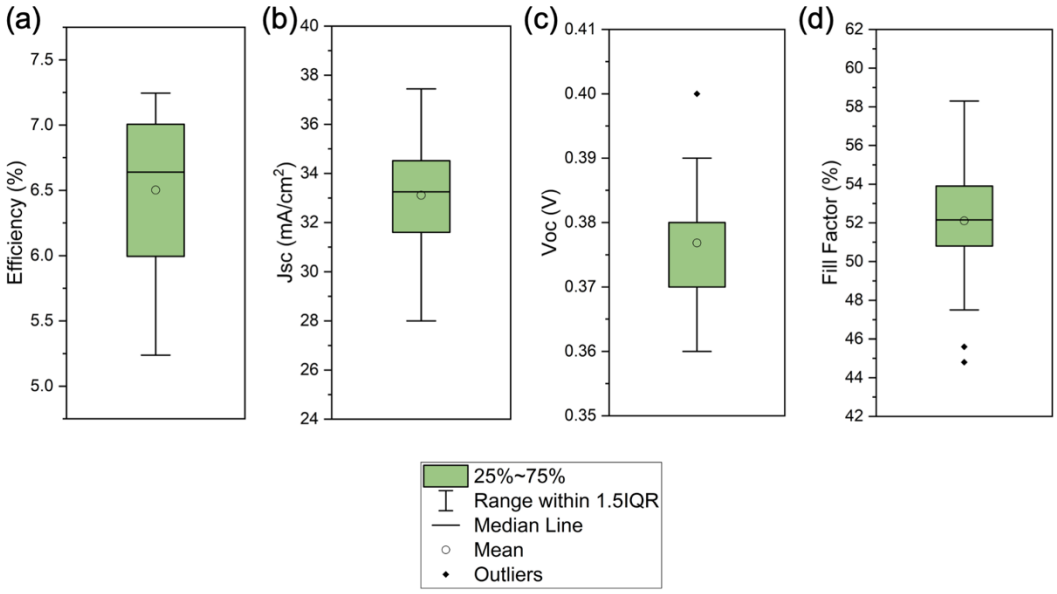

Figure S12. a) Efficiency, b) short circuit current (Jsc), c) open circuit voltage (Voc), and d) fill factor (FF) distributions for the 22 $CuInSe_2$ solar cells fabricated from the Cu-In-BAPSe inks.

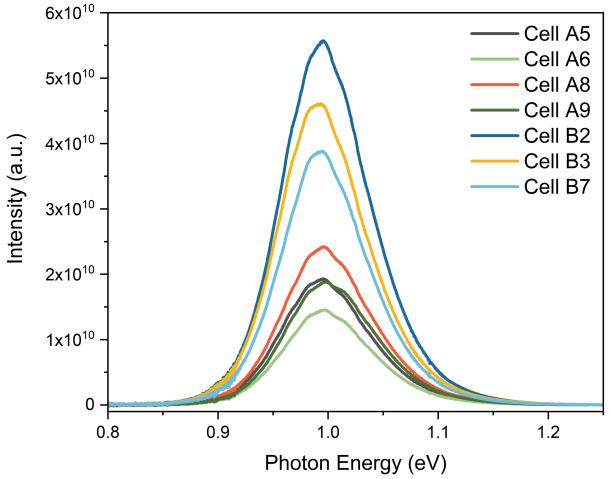

Figure S13. Photoluminescence spectra for $CuInSe_2$ absorber layers in the fabricated devices.

Application of Alkylammonium Polyselenides to Nanomaterial Synthesis

In addition to the synthesis of $CuInSe_2$ nanoparticles, the alkylammonium polyselenide inks could also be used to synthesize binary nanoparticles. Utilizing the previously described process for $CuInSe_2$, the separate copper and indium polyselenide inks were used in the synthesis of copper selenide and indium selenide. When using the copper polyselenide solution, XRD (Figure S14.a) identified the resulting material as being crystalline $CuSe_2$, while TEM (Figure S14.b) revealed particle sizes on the order of 1 micron, making these microparticles rather than nanoparticles. The resulting material obtained from the indium polyselenide solution was not easily identified. XRF provided a Se/In ratio of about 2.3 and the obtained Raman spectra (Figure S14.c) could not be matched to InSe or In_2Se_3. Interestingly, TEM (Figure S14.d) revealed the formation of nanorods which were also observed to fluoresce green light (Figure S14.e).

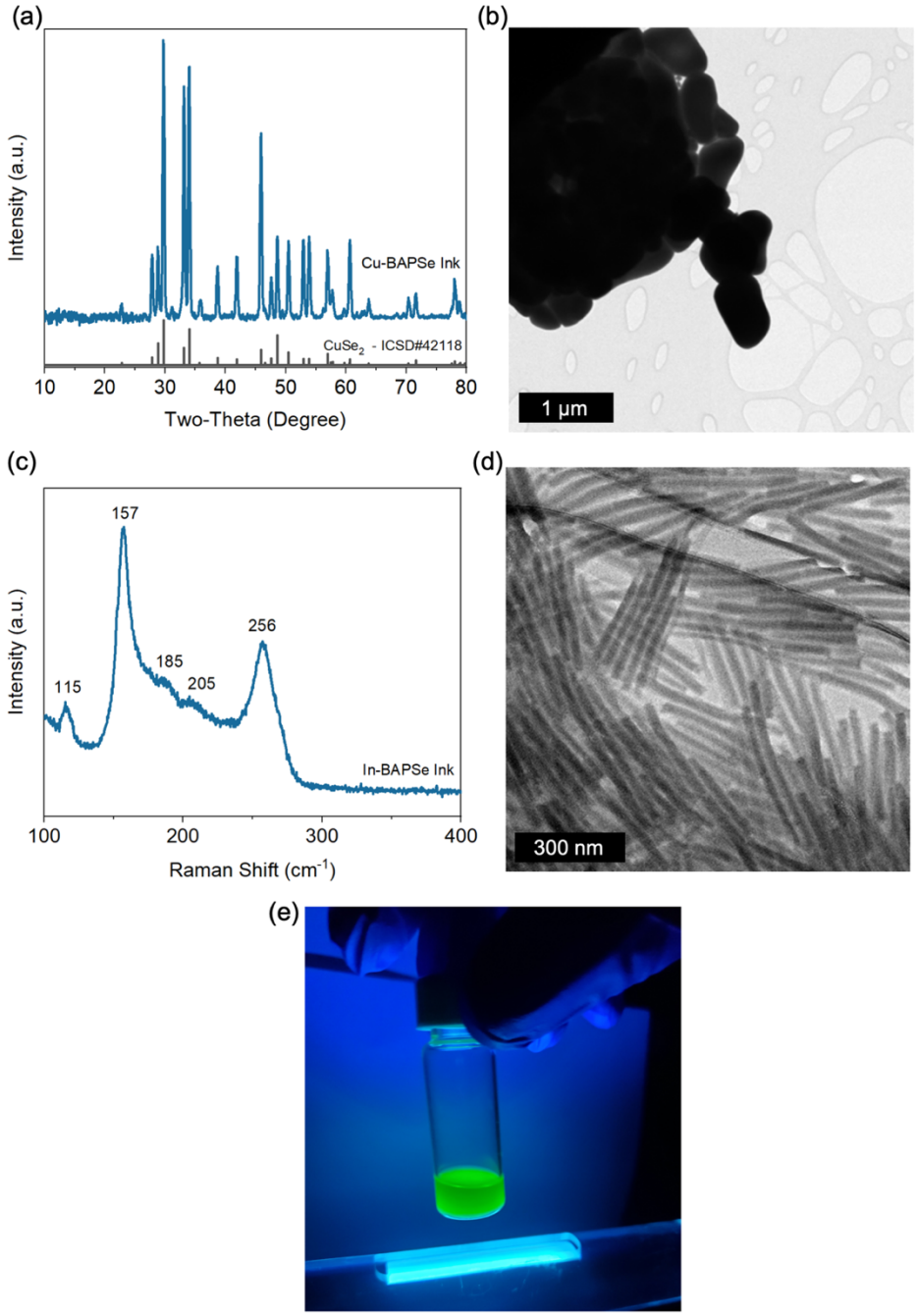

Figure S14. a) XRD spectrum and b) TEM image for the microparticles obtained utilizing copper polyselenide as a precursor. c) Raman spectrum and d) TEM image for the nanorods obtained utilizing indium polyselenide as a precursor. e) Photograph showing the green fluorescence of the indium selenide nanorods under ultraviolent illumination.

References

1 C.-H. Chung, S.-H. Li, B. Lei, W. Yang, W. W. Hou, B. Bob and Y. Yang, Identification of the Molecular Precursors for Hydrazine Solution Processed $CuIn(Se,S)_2$ Films and Their Interactions, *Chem. Mater*, 2011, **23**, 964–969.

2 S. S. Dhingra and M. G. Kanatzidis, Polyselenide Chemistry of Indium and Thallium in Dimethylformamide, Acetonitrile, and Water. Syntheses, Structures, and Properties of the New Complexes $[In_2(Se_4)_4(Se_5)]^{4-}$, $[In_2Se_2(Se_4)_2]^{2-}$, $[In_3Se_3(Se_4)_3]^{3-}$, and $[Tl_3Se_3(Se_4)_3]^{3-}$, *Inorg. Chem.*, 1993, **32**, 1350–1362.